

A stronom y & Astrophysics manuscript no.  
(will be inserted by hand later)

## Optical and near infrared observations of V1647 Ori and McNeil's Nebula in February{April 2004

M. Kun<sup>1</sup>, J.A. A costa{Pulido<sup>2</sup>, A. M oor<sup>1</sup>, P. Abraham<sup>1</sup>, M. Charoos{Llorens<sup>2</sup>, A. K ospal<sup>3</sup>,  
Sz. C szm adia<sup>1</sup>, A. M anchado<sup>2</sup>, M. J. V idal{Nunez<sup>2</sup>, and J.M. Benkó<sup>1</sup>

<sup>1</sup> Konkoly Observatory, H-1525 Budapest, P.O. Box 67, Hungary

<sup>2</sup> Instituto de Astrofísica de Canarias, E-38200, La Laguna, Tenerife, Canary Islands, Spain

<sup>3</sup> Department of Astronomy, Lorand Eotvos University, H-1518 Budapest, P.O. Box 32, Hungary

Received / Accepted

**Abstract.** We combine our V, R, I, J, H, K<sub>s</sub> photometric and near infrared spectroscopic observations of the outburst star V1647 Ori obtained in the period 12 February{24 April 2004 with published data in order to make inferences on the geometry of the object and the nature of the eruption. The main results are as follows: (1) Our photometric results do not indicate systematic fading of the star in the period of observations. (2) Assuming a spectral type A0 in the visual wavelength regime, the observed R<sub>c</sub> - I<sub>c</sub> colour index of the star yields a reddening A<sub>V</sub> = 8.4 mag, and with this A<sub>V</sub> the mean observed V = 17.4 mag corresponds to M<sub>V</sub> = 1.0 mag. (3) Examination of the time delay between the brightness variations of the star and two nebular positions allowed us to derive an angle of about 60° between the axis of the nebula and the line of sight. (4) Comparison of the K<sub>s</sub> and R<sub>c</sub> images of McNeil's nebula shows that HH 22A consists of two physically different knots: the southern is a part of the nebula but not seen in the K<sub>s</sub>, while the northern one is outside the illuminated region, but exhibits H<sub>2</sub> 2.12 μm emission. (5) The J - H and H - K<sub>s</sub> colour maps of the infrared nebula, which trace the density structure of the circumstellar environment of V1647 Ori, reveal a flattened envelope whose main axis, about 20° (0.04 pc) in size, is perpendicular to the axis of the optical nebula. (6) As an explanation for the lack of shock signatures in the spectrum of V1647 Ori, we propose that, instead of dust removal from the line of sight to the star by stellar winds, the appearance of a new, hot source, exhibiting the observed B(A type spectrum, accounts for both the illumination of the nebula and the colour and brightness variations of the star. (7) No clear evidence of magnetospheric accretion, characteristic of EXors, can be identified in the published optical and near infrared spectra of the star. On the contrary, several features characteristic of FUors do appear. Together with the light curve and SED the spectroscopic properties suggest that V1647 Ori is an FU Ori type star.

**Key words.** stars: formation{stars: circumstellar matter{stars: individual: V1647 Ori { stars: pre-main sequence{ISM : individual objects: McNeil's nebula

### 1. Introduction

The young star (IRAS 05436 0007, LMX 12, McNeil's Nebula Object, V1647 Ori) whose outburst produced McNeil's nebula offers a unique opportunity to study phenomena accompanying the strong brightening of a low-mass pre-main sequence star. Both known types of outburst objects, FUors and EXors are very rare to build a consistent view on the physics of the events, therefore any new eruption, like the one of V1647 Ori in January 2004 (McNeil 2004) attracts a number of observers.

By the end of the first observing season after the outburst (January{May 2004), several observational results have been published, but the various phenomena observed during the short time span of the post-outburst

evolution have not yet resulted in a consistent picture of the outburst. The first observational data on the optical and infrared spectra and on the colour change of the object illuminating the new reflection nebula (Reipurth & Aspin 2004) led to the conclusion that the star, later designated as V1647 Orionis (Samus 2004), differs from the known FUors in several respects. Contrary to FUors, strong H<sub>2</sub> emission line could be seen in the optical spectrum, and Br<sub>2</sub> and CO emission in the near infrared.

On the contrary, Bríceño et al. (2004) recalled that the prototypical FUor V1057 Cygni displayed a strong H<sub>2</sub> emission immediately after its outburst which turned into the characteristic absorption with P Cygni profile several years later (Herbig 1977). The optical spectrum of V1647 Ori, detected in the light reflected from the nebula by Bríceño et al. (2004) in February 2004, showed an early

A or even B type star, incompatible with the EX or nature. The near infrared spectrum of V1647 Ori taken early March exhibited several emission features (Vacca, Cushing & Simon 2004). The hydrogen Paschen and helium lines present P Cygni profiles, indicative of high velocity winds. Both the pre- and post-outburst infrared spectral energy distributions of the star (Abraham et al. 2004, Andrews et al. 2004) suggest that the outbursting star was a fast spectrum object. Optical and near infrared photometry, spanning three months after the outburst, presented by Walter et al. (2004) indicated a steady decline of 0.3–0.4 mag.

The colour change of the star during the outburst led Reipurth & Aspin (2004) to propose that a strong stellar wind, clearing the line of sight around the star, played a role in the brightening of both the nebula and the star. However, no spectroscopic signature of the collision of the wind with the circumstellar gas has been found in the spectrum of V1647 Ori (Reipurth & Aspin 2004; Andrews, Rothberg & Simon 2004). A reason for this may be that forbidden lines, formed in the shocked gas, are de-excited by collisions in the dense circumstellar gas (Vacca et al. 2004).

In this paper we present results of our imaging photometric observations in the period 12 February–24 April 2004, as well as the near infrared spectrum of the star obtained on March 8 using the new infrared instrument LIRIS installed on the William Herschel telescope. Together with published observations, performed with various instruments, our data may contribute to understand better the nature of the object. Our observations and data reduction are described in Sect. 2. The results of the observations are presented in Sect. 3. We discuss our data in conjunction with published results in Sect. 4, and a short conclusion is given in Sect. 5.

## 2.0 Observations and data reduction

### 2.1 Optical imaging and photometry

We observed V1647 Ori and its environment using the 60/90 cm Schmidt telescope of Konkoly Observatory on 12 and 16 February as well as 1 and 2 April 2004 in the Johnson V and Cousins R<sub>c</sub> and I<sub>c</sub> colours. The detector was a Photometrics AT 200 CCD camera, having a pixel size of 9 μm, corresponding to 1°03 on the sky. We also observed the object with the 1 m RCC telescope of Konkoly Observatory on 20 February in the R<sub>c</sub> and I<sub>c</sub> bands and on 6 March in the I<sub>c</sub>, using the Princeton Instruments Versarray 1300B camera, whose pixel size of 20 μm corresponded to 0°306 on the sky. We also obtained V, R<sub>c</sub> and I<sub>c</sub> images using the IAC 80 cm telescope at the Teide Observatory on 22 and 24 April 2004. The camera contains a 1024 × 1024 Thomson CCD detector, with a scale of 0°433/pixel. The journal of the optical imaging observations is given in Table 1.

The reduction procedures, including bias-subtraction, flat-fielding and cosmic ray removal, was done in IRAF.

The wide fields of Konkoly observations (17°5°–26°4° for the Schmidt and 6°–6° for the RCC telescope, respectively) allowed us to determine the point spread functions of the images. The instrumental magnitudes of V1647 Ori were determined by psf photometry using the IRAF 'allstar' task. 18 field stars were used for determining the psf of the images obtained with the Schmidt telescope, whereas 10 stars were available for this purpose in the RCC images. The internal error of the photometry was < 0.01 mag. Three comparison stars, located within the observed field, were used for establishing the zero-point shift between the instrumental and standard magnitudes. V, R<sub>c</sub> and I<sub>c</sub> magnitudes of these stars were listed by Henden (2004). We recalibrated these stars during our observing run on 24 April (photometric night). The computed magnitudes of the comparison stars are shown in Table 2. The optical observations obtained at IAC 80 on 24 April were calibrated by observing the stars 556/557/563 in the standard field SA 98 from Landolt's (1992) compilation. Due to the small field of view we had not enough stars for psf photometry, therefore we performed aperture photometry on the IAC 80 cm images, using an aperture of 4°5 radius.

### 2.2 Near infrared imaging

J, H, and K<sub>s</sub> images were obtained on 4 March 2004, during the second commissioning period of the new infrared instrument LIRIS (Acosta-Pulido et al. 2003; Manchado-Torres et al. 2003) installed on the 4.2 m William Herschel Telescope at the Observatorio del Roque de Los Muchachos. The detector was a 1024 × 1024 Hawaii-1 chip. For both the J and H bands we took 6 individual frames of 20 s each following a 5-point dither pattern. For the K<sub>s</sub> band we took 8 individual frames of 10 s each, following a 8 point dither pattern. The frames were taken using double correlated readout mode. The exposure times of the individual frames were selected in order to have good S/N across the nebula, which causes entering the non-linear regime, or even strong saturation in the H band image, of the detector at the position of the illuminating star of the nebula. The usual dithering technique was used in order to eliminate the sky emission. The images were reduced using the package 'liris.q1' developed in the IRAF system. The photometric calibration was done using five stars with known infrared magnitudes in the 2MASS All Sky Catalogue (IPAC 2003). In order to measure the flux of the illuminating star we have parametrized the PSF as a model profile by looking at field stars. Later we fit the non-saturated parts of the star profile using the previously determined profile and estimate the flux of the star.

We also obtained J and H band observations with the 1.52 m Carlos Sanchez Telescope at the Teide Observatory on 21 March 2004. The infrared camera (CAIN) is equipped with a 256 × 256 Nicon 3 detector, which provides a pixel projection of 0°40 with its narrow optics con-

Table 1. Journal of the photometric observations (optical and near IR imaging)

Date	Telescope	Scale ("/pix)	Filter	Exptime (s)	Filter	Exptime (s)	Filter	Exptime (s)
2004 02 12	Schmidt	1.03	V	120	R <sub>c</sub>	120	I <sub>c</sub>	120
2004 02 16	Schmidt	1.03	V	360	R <sub>c</sub>	360	I <sub>c</sub>	360
2004 02 20	RCC	0.306	R <sub>c</sub>	540	I <sub>c</sub>	540		
2004 03 04	WHT	0.25	J	1200	H	600	K <sub>s</sub>	640, 32
2004 03 06	RCC	0.306	I <sub>c</sub>	300				
2004 03 21	TCS	0.40	J	500	H	350		
2004 04 01	Schmidt	1.03	I <sub>c</sub>	600				
2004 04 02	Schmidt	1.03	V	2400	R <sub>c</sub>	1200	I <sub>c</sub>	900
2004 04 22	IAC 80cm	0.4325	V	600	R <sub>c</sub>	200	I <sub>c</sub>	600
2004 04 24	IAC 80cm	0.4325	V	600	R <sub>c</sub>	600	I <sub>c</sub>	600

Table 2. Data of comparison stars

Star	RA (2000)	Dec (2000)	V	R <sub>c</sub>	I <sub>c</sub>
a	05 46 22.40	00 03 38.1	15.651 (0.015)	14.908 (0.006)	14.262 (0.005)
b	05 46 22.43	00 08 52.6	15.124 (0.013)	14.156 (0.005)	13.216 (0.005)
c	05 46 00.25	00 08 26.2	16.914 (0.065)	15.485 (0.006)	13.820 (0.005)

guration. The journal of the optical imaging observations is given in Table 1.

### 2.3. Near infrared spectroscopy

Two spectrograms of V1647 Ori were obtained with LIRIS on 8 March 2004, covering the wavelength intervals of 0.9–1.4 μm and 1.4–2.4 μm, with exposure times of 400s and 12s, respectively. The spectra were reduced and calibrated using the package "irisql" developed within IRAF platform. In order to reduce the readout noise, the frames were obtained using multiple correlated readout mode, with 4 readouts before and after the integration. We used a slit width of 1" which yielded a spectral resolution of 410 and 510 in the ZJ and HK spectra, respectively. Finally, one dimensional spectra were extracted with the IRAF "apall" task. We use observations of the A0 V star HIP 28056 to correct for telluric features in the spectra.

## 3. Results

We present our results for the outburst star V1647 Ori and its illuminated nebula separately.

### 3.1. Results on V1647 Ori

#### 3.1.1. Photometric behaviour

The results of our photometry of V1647 Ori are listed in Table 3. Most of the photometric errors, given in parentheses, derives from the error of the magnitude shifts between V1647 Ori and the three comparison stars, because

the colour dependence of these shifts could not be determined. The light curve in the I<sub>c</sub> band is displayed in Fig. 1. Our photometric measurements, performed in the V, R<sub>c</sub> and I<sub>c</sub> bands are distributed over a period of 72 days. Our data do not indicate appreciable fading of the star during this period, although fluctuations in the brightness and colours over the formal errors can be recognized. On the other hand, Walter et al. (2004) claimed a general decline of the optical brightness, based on a much larger data set. The general impression is that their last two data points biased that conclusion. Any long term variation has to be confirmed with new data spanning a much longer time period.

Our near infrared photometry covers only a short time period (17 days). Comparison with other post-outburst measurements (Reipurth & Aspin 2004; Ojha et al. 2004; Vacca et al. 2004) again shows no systematic fading of the near infrared brightness. The most recent dataset presented by Walter et al. (2004) apparently showed a slow but steady decline of V1647 Ori in the K band.

#### 3.1.2. The near infrared spectra obtained with LIRIS

The LIRIS spectra in the ZJ and HK bands, normalized to their continua, are shown in Fig. 2. The most important spectral lines of the regions are marked in the figure. Comparison of the K-band spectrum with that of Reipurth & Aspin (2004), obtained a month earlier shows no appreciable change in its appearance between 3 February and 8 March. Our spectra were taken on March 08, 21.6h UT, while the spectrum discussed by Vacca et al.

Table 3. Results of optical and near infrared photometry of V1647 Ori in February (April 2004)

Date	JD 2,453,000+	V	$R_c$	$I_c$	J	H	$K_s$
2004 02 12	048.3		16.11 (0.13)	14.40 (0.08)			
2004 02 16	052.3	17.43 (0.08)	16.35 (0.21)	14.42 (0.12)			
2004 02 20	056.3		17.09 (0.09)	14.71 (0.08)			
2004 03 04	069.4				11.13 (0.1)	9.40 (0.2)	7.44 (0.1)
2004 03 06	071.3			14.59 (0.15)			
2004 03 21	086.3				10.91 (0.05)	8.83 (0.05)	
2004 04 01	097.2			14.83 (0.06)			
2004 04 02	098.3	16.83 (0.12)	16.09 (0.08)	14.57 (0.06)			
2004 04 22	118.4	17.30 (0.10)	15.98 (0.10)	14.30 (0.08)			
2004 04 24	120.3	17.84 (0.16)	16.156 (0.034)	14.381 (0.03)			
2004 04 24	120.3	17.491 (0.064)	15.979 (0.013)				

In these nights the star cannot be identified as a point source in the V images. The magnitude given results from aperture photometry at the position of the star as defined by Briceño et al. (2004).

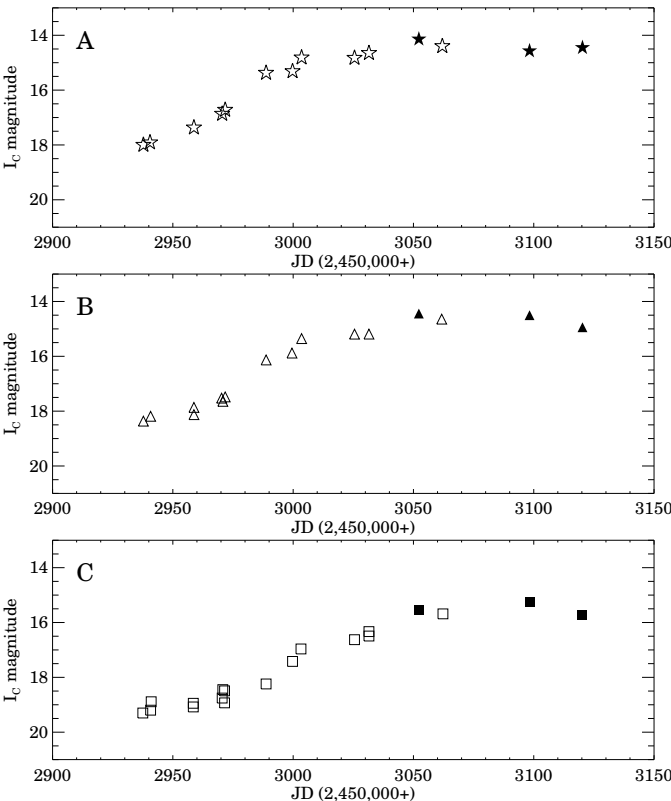


Fig. 1. Briceño et al. (2004) light curves (open symbols) of V1647 Ori (A) and positions B and C of the McNeil's Nebula, supplemented with our observed magnitudes (filled symbols). While the brightness of the star shows no overall fading, the nebular points were fainter on 24 April.

(2004) was obtained only a few hours later, on March 09, 06h UT. Differences between them are expected mainly due to the lower spectral resolution of our spectra and the

Table 4. Equivalent widths of emission lines observed by LIRIS in the near infrared spectrum of V1647 Ori

Line	EW (m)	EW (Å)
Pa	1.005	0.8 (0.1)
HeI	1.083	8.2 (1.0)
Pa	1.094	4.9 (0.4)
Pa	1.282	9.8 (0.5)
Pa	1.875	35.0 (3.0)
Br	1.945	2.8 (0.2)
Br	2.166	10.0 (1.5)

smaller S/N ratio in the HK spectrum obtained with a very short integration time.

The most prominent features seen in the spectra are several H recombination bright emission lines (Pa, Pa, Br), the CO bands in emission and a strong HeI absorption line at 1.083 m (it will be discussed in more detail in Sect. 4.3). A remarkable feature of the H-band part of the spectrum, not shown by Vacca et al. (2004), is that while Br10, Br11 and lower order transitions can be seen in emission, Br15 is clearly detected in absorption (see the inset in Fig. 2). A similar situation was observed in the Balmer lines by Briceño et al. (2004): H and H appear in emission, and the higher order lines, beginning from H are seen in absorption. Brackett lines in absorption are indicative of B and A type stellar photosphere (Lançon & Rocca-Volmerange 1992). Like the high order Balmer lines, the Br15 absorption may originate from the hottest and densest regions of the star/disk system.

Equivalent widths of the most prominent hydrogen and helium lines are listed in Table 4. The typical uncertainty of the equivalent widths, estimated from repeated measurements, is about 10%. The resulting values are consistent with those presented by Vacca et al. (2004).

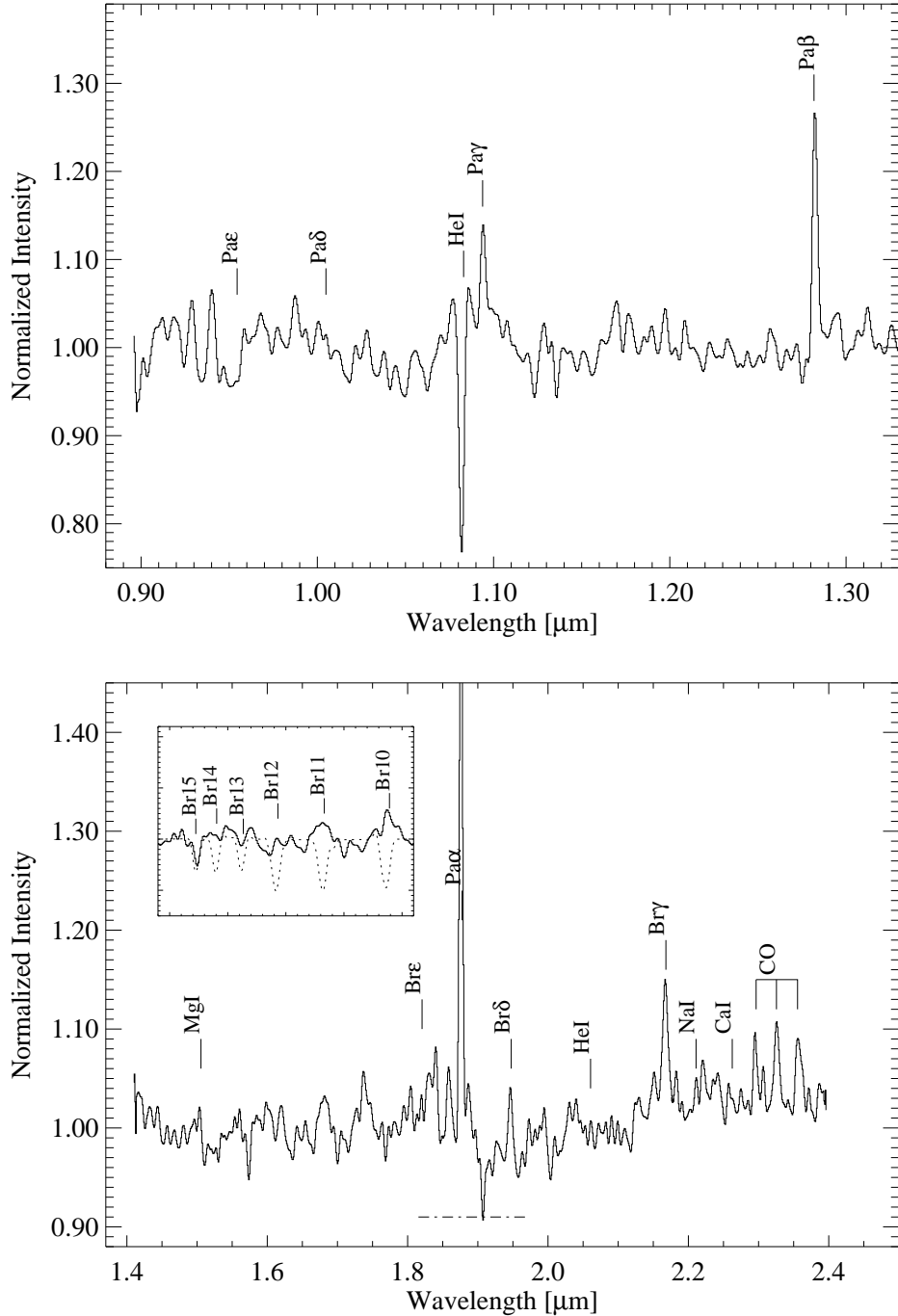


Fig. 2. Near infrared spectrum of V 1647 Ori obtained with LIRIS, normalized to the continuum. Upper panel: ZJ band; lower panel: HK band. The position of several important lines ( $\text{Pa}\alpha$ ,  $\text{Br}\epsilon$  and  $\text{Br}\gamma$ ) coincides with the spectral range where telluric absorption is very strong (marked by the horizontal dashed line). The small inset shows a comparison with the telluric correction star H IP 28056, just to show how the  $\text{Br}$  lines change their profile.

### 3.2. Results on McNeil's Nebula

#### 3.2.1. Morphology

Figure 3 shows the  $R_c$  and  $K_s$  images of the nebula projected on each other. The optical image was taken on Feb 20, whereas the  $K_s$  image was observed in March 4. The

lowest significant  $K_s$  contours are plotted in the figure in order to indicate the outer boundary of the nebula. The shape of the optical nebulosity delineates the polar outflow cavity of the star, the star V 1647 is located at the apex of the nebula and there is no optical emission on the southern side. The bluest part of the nebula is detected as a plume at about 60 arcsec towards the North-West (see

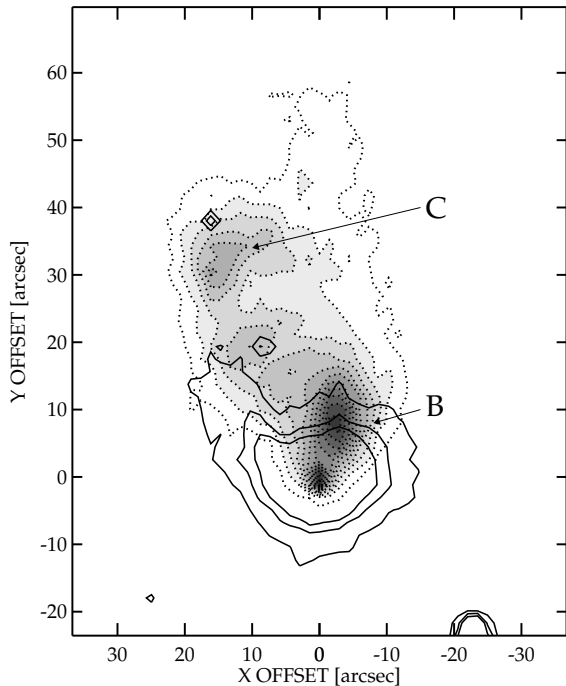


Fig. 3. M cNeil's nebula in the  $R_c$  (dotted line and shading), observed on Feb 20 with the 1m RCC telescope of Konkoly Observatory, and the lowest contours of the  $K_s$ , as observed on March 4 with the William Herschel Telescope. Positions B and C of the photometric measurements are indicated. Notice that HH 22 at the offsets [16,36] splits into two parts.

Fig. 1 of Reipurth & Arp (2004). The morphology observed in the  $K_s$  band is very different showing a roughly spherical nebula, with some extension to the north-east along the wall of the cavity and the star near its centre. The blue plume is not present in our near IR images, except as a faint extension in the J band. The mean angular size of the infrared nebula, about  $25''$ , corresponds to a linear extent of 0.05 pc at a distance of 400 pc.

In addition to the spherical dusty envelope around the star, a conspicuous feature of the  $K_s$  image is the northern part of knot A of HH 22 (Eislösel & Mundt 1997, their Fig. 10) at the offset [16'', 38''], which appears in the  $K_s$  image due to its emission of the  $H_2$  line at 2.12  $\mu$ m. On the contrary, the southern, larger lobe of HH 22A, which coincides with clump C of M cNeil's nebula, cannot be seen in the 2.12  $\mu$ m  $H_2$  line. Thus HH 22A, a coherent object in Eislösel & Mundt's (1997) [SII] image, splits into two physically different parts. Bríceño et al. (2004) have shown that HH 22A brightened during the outburst. However, this is true only for the southern part of the knot. The northern part, observed in the infrared, lies outside the illuminated cavity.

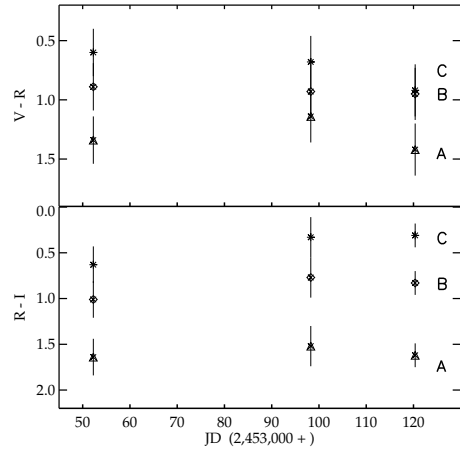


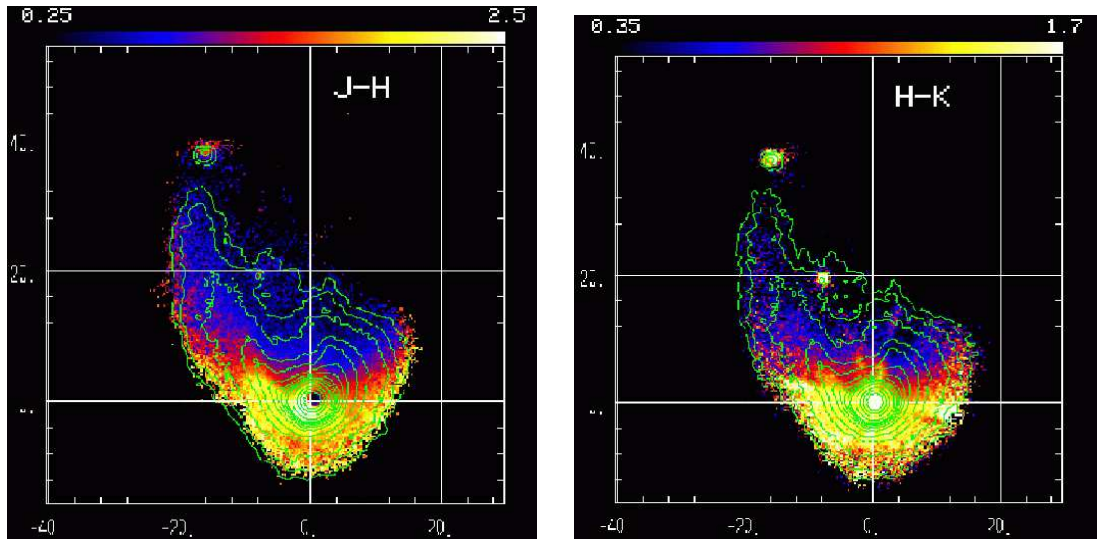
Fig. 4.  $V - R_c$  and  $R_c - I_c$  colours of M cNeil's Nebula at positions B and C. For comparison, the colours of V 1647 Ori (A) are also plotted.

### 3.2.2. Optical brightness and colours of the nebula

M cNeil's nebula shines due to the scattered light of V 1647 Ori, therefore its observed properties are closely related to the brightness of the star and to the structure and geometry of its circumstellar environment. Bríceño et al. (2004) established a time delay between the brightening of the star and two well-defined positions of the nebula. Positions B and C are defined by their angular distances from the star 2MASS J05461889 0005381 (denoted as star V by Bríceño et al. 2004). Moreover, the composite optical,  $g^0, r^0, z^0$  image presented by Reipurth & Arp (2004) has shown the nebula bluer at the regions farther from the star, which may reflect variation of dust column density across the surface of the nebula. The morphology of the nebula with its apex at the illuminating star V 1647 Ori is also consistent with the optical emission purely attributed to scattered light. In order to quantify the colour distribution and obtain further data on the nature of the variability of the nebula we measured the  $V$ ,  $R_c$ ,  $I_c$  magnitudes within circular apertures centered on the positions B and C and calibrated their magnitudes against the comparison stars listed in Table 2. In order to have results comparable with those in Bríceño et al. (2004), in spite of the different image scales and psf widths, the aperture radii are defined as  $a^2 = (FWHM)^2 + r^2$ , and  $r = 4''$ , same as used by Bríceño et al. (2004). We give the photometric results for these positions of the nebula in Table 5. The  $V - R_c$  and  $R_c - I_c$  colour indices of the star and the nebula, measured on 16 February, 2 April and 24 April, are displayed in Fig. 4. These results will be discussed in Sect. 4.1.

Table 5.  $V$ ,  $R_c$  and  $I_c$  magnitudes of B and C positions of McDonald's Nebula in February/April 2004

Date	Pos.	V	R	I	V	R	I	
		(0.08)	(0.21)	(0.12)	0.89	1.01	0.60	0.63
2004 02 16	B	16.34	15.45	14.44	0.89	1.01	0.60	0.63
	C	16.78	16.18	15.55	0.93	0.77	0.68	0.33
2004 04 02	B	16.20	15.27	14.50	0.95	0.83	0.92	0.31
	C	16.25	15.78	15.25	0.95	0.83	0.92	0.31
2004 04 24	B	16.72	15.77	14.94	0.95	0.83	0.92	0.31
	C	16.97	16.05	15.74	0.95	0.83	0.92	0.31

Fig. 5. Maps showing the  $J - H$  (left panel) and  $H - K$  (right panel) colours of the infrared nebula around V 1647 Orionis. The absolute colours have been obtained by comparison with 2MASS. The axes are in arcsec.

### 3.2.3. Near infrared colours of the nebula

The  $J$ ,  $H$  and  $K_s$  images obtained with LIRIS were used to derive the  $J - H$  and  $H - K$  colour maps of the nebula. The absolute colour has been obtained by comparison with 2MASS as mentioned above. The resulting colour maps are shown in Fig. 5. It can be seen that the nebula appears much redder at the south of the illuminating star outlining a flattened region or D shape structure, whose elongation is nearly perpendicular to the axis of the optical nebula. The largest apparent diameter of this structure is  $18''$ . The nebula changes rapidly to bluer colours when crossing the central part towards North.

The colour structure seen in the infrared nebula could be interpreted by two different scenarios: a large extinction is present in the equatorial plane of the illuminating star-nebula system or there is an infrared excess in the  $K_s$  band due to hot dust emission. The presence of extended near-IR emission in excess of scattered starlight has been claimed by Sellgren et al. 1996. These authors attributed the emission to very small dust grains transiently heated to high temperatures. We show in Fig. 6 a colour-colour diagram with representative values of the North, equatorial and South parts of the nebula. In the same figure we

present the reddening vectors starting from the bluest part (North) and the loci of reflection nebulae with extended emission in Sellgren's et al. (1996) work. It can be seen that the equatorial and southern regions are very red and fall near the reddening track, they lie at  $A_V = 7.5$  and  $A_V = 12$ , respectively. On the other hand they also lie very close to the loci of blackbody emission, the southern region can be interpreted as emission at  $T = 1200$  K, and the equatorial region could be a mixture of dust emission plus a scattering contribution. From these data we cannot rule out any of the scenarios. In any case we have found evidence of a dusty disk structure at the equatorial plane of the star-nebula system.

## 4. Discussion

### 4.1. Geometry and appearance of the optical nebula

Brieno et al. (2004) estimated a time delay  $\sim 50$  days between the brightness variations of V 1647 Orionis and the changes in brightness of position C of the nebula, while the corresponding delay between position B and the star was about 14 days. The exact definition of the nebular positions allowed us to supplement their long-term light

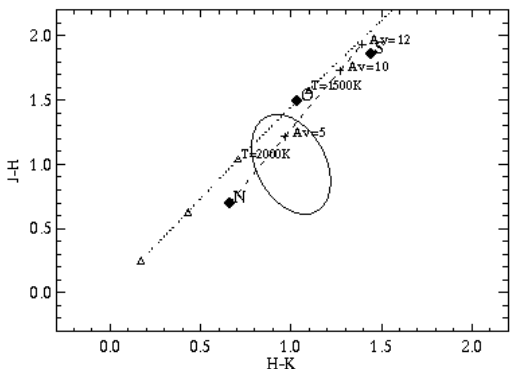


Fig. 6. Near infrared colour-colour diagrams showing the location of representative regions (N (North); O (Equatorial); S (South)). The dashed line represents the reddening vector corresponding to different values of  $A_V$ . The dotted line represents the loci of blackbody emission. The ellipse marks the region corresponding to reection nebulae showing dust emission as claimed by Sellgren et al. (1996).

curves with our photometric data and use these curves for a more accurate determination of the time delays between them. We show the light curves expanded by our points in Fig. 1. The brightness of the star shows no overall fading, while both nebular points were fainter on 24 April.

We reanalysed the three I<sub>c</sub>-band light curves in order to find the accurate time shifts between them. First we resampled the light curves so that the time resolution was 0.25 days. The resulting light curves of V1647 Ori, position B and position C are called A ( $t_i$ ), B ( $t_i$ ) and C ( $t_i$ ), respectively, where  $t_i$  is time ( $i = 1 \dots N$ ). Then we calculated a function called D (s) as follows:

$$D(s) = \frac{\sum_i A(t_i) C(t_i) s}{\sum_i A(t_i) C(t_i)}$$

The s which results in the lowest value of D (s) gives the time shift between the light curves of A and C. The time delays between A and B as well as A and C were calculated, resulting in the following values:  $14^{+1.5}_{-2.0}$  days at region B and  $50^{+3.0}_{-3.0}$  days at region C.

The time shift of 50 days between the light curves of region C and the illuminating star receives support from Walter et al.'s (2004) light curve, displaying a prominent dip between 5 and 7 March, 48{50 days before our detection of the decline at C. Taking into account that the apparent size of clump B is comparable with its angular distance from the star, the decline observed at A on 24 April may be connected to the dip in Walter et al.'s (2004) light curve on April 12. Thus our results confirm that the light from region C (H II 22a south) is indeed the light echo from V1647 Ori.

The measured time delay between the light curves of A and C, together with the projected separation of the two objects results in an inclination of 60° for the axis of the nebula with respect to the line of sight. This angle also

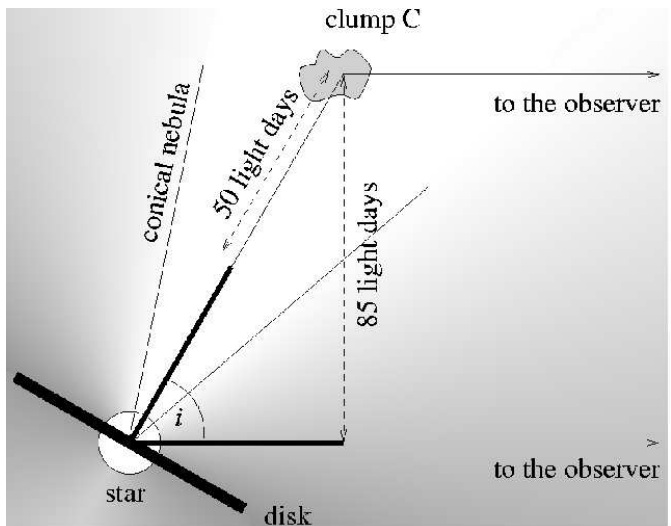


Fig. 7. Geometry of McNeil's nebula, deduced from the time delay between the light curves of V1647 Ori and Clump C.

serves as an estimate on the inclination of the rotation axis of the star. The time delay between A and B results in 73°. The difference of 10 degrees can be interpreted as result of the 3-D structure of the nebula, which has to be confirmed by other time delay measurements. The result suggests that the illuminated cavity opens slightly towards us. Figure 7 shows the schematic view of the star-disk-nebula system.

#### 4.2. Structure of the circumstellar environment

Having estimated the inclination of the nebular axis to the line of sight the structure of infrared colour maps (Fig. 5) is easy to understand. If we suppose that the scattering properties of the dust are the same across the nebula, then the observed colours reflect the amount of the scattering dust between the light source and the observer. The north/south asymmetry of the colour maps results from the inclination. The attenuated structure of the most heavily reddened part of the infrared nebula can be identified as a dusty envelope of the star. The largest apparent size of this structure,  $18^{10}$ , corresponds to 0.029 pc or 7000 AU, the same as the size derived by Johnstone et al. (2001) for the coinciding submillimeter source Orion B-mm 55. We observe the light of the central object in this direction scattered by the same dust which radiates at the submm wavelengths.

The winds from the star/disk system, accompanying the accretion, opened a cavity towards north and towards us into this envelope. The southern lobe of the outflow can be recognized in the southernmost part of the infrared nebula. The extinction along its line of sight is much higher than the corresponding value towards the northern lobe. This structure is very similar to the infrared nebula of S140, studied by Harker et al. (1997).

The colour indices measured at position C suggest that the reflected light suffers an extinction of  $A_V = 2.7$  mag, if the light of an A0 type star is reflected from this dust clump ( $R_c = I_c = 0$ ). Most of this extinction occurs between the position C and us, within the Orion B cloud.

#### 4.3. On the nature of the outburst

A remarkable feature of the outburst of V1647 Ori is that its J – H and H – K colours changed precisely along the reddening line, suggesting that the total change in the colours and part of the brightening resulted from a decrease in the extinction. Reipurth & Aspin (2004) estimated that the visual extinction diminished by some 4.5 magnitudes.

Involving the pre- and post-outburst  $I_c$  magnitudes into the studies the colour change seems to confirm the picture of the decreasing extinction. Figure 8 shows the path of the star in various colour-colour diagrams based on our post-outburst and published pre-outburst (2MASS; Barricero et al. 2004) data. The reddening slopes are from Cohen et al. (1982) and Rieke & Lebofsky (1985).

Figure 8 suggests that the colour changes of V1647 Ori can readily be explained with a decrease of some 5 mag in the visual extinction. However this picture has some physically implausible consequences. First, if the extinction decreased due to the stellar winds, then the column density of the molecular material pushed aside during the outburst should be very large: about  $4.5 \times 10^{21} \text{ cm}^{-2}$ . Absence of shock signatures in the spectrum of the star contradicts this picture. Moreover, this hypothesis postulates a colour-independent intrinsic brightening of 2.4 mag of the star in each photometric band.

In order to avoid these difficulties we propose a different scenario to explain why the source evolved along the reddening paths. As both decreasing extinction and increasing temperature result in bluer colours, appearance of a hot light source in the line of sight could produce the same colour changes as dust removal. The observed B (A type spectrum of the light reflected from the star and the presence of the strong helium line indicate that hot regions did appear in the star/disk system during the outburst. The sizes and temperatures of the hot components together with the reddening of the system can combine so that their effect on the observed colours is decreasing extinction. This is illustrated by the simple model given by Walter et al. (2004), approximating the optical and near infrared parts of the post-outburst SED with two reddened blackbodies. During a real outburst various regions of the star and its disk are probably heated to different temperatures, the hottest of which are the regions of the accretion shock. The intrinsic brightening of the star/disk system, accompanied by an increase of the temperature, can equally explain the illumination of the nebula and the colour and brightness variations of the star. If we assume that the visual extinction remained unchanged during the outburst, then the amplitudes of the intrinsic

brightening of the star were  $I = 5.4$  mag,  $J = 3.7$  mag,  $H = 3.2$  mag, and  $K_s = 2.8$  mag.

We estimated the extinction suffered by V1647 Ori from the E ( $R_c = I_c$ ) colour excess, which is usually regarded to be a good tracer of the reddening (Meyer et al. 1997). In estimating the E ( $R_c = I_c$ ) we assumed  $(R_c - I_c)_0 = 0$  and used the relation

$$A_V = 4.75 \times E(R_c - I_c);$$

(Cohen et al. 1982). Thus we obtained  $A_V = 8.4$  mag, somewhat lower than the  $A_V = 11$  mag estimated by Vacca et al. (2004) from the optical depth of the 3 mm feature. The V magnitude of the star, corrected for this extinction and assuming a distance of 400 pc, corresponds to an absolute magnitude  $M_V = 1.0$ , that is, the post-outburst luminosity in the V band is  $L_V = 25 L_\odot$ .

An important clue to the nature of the outburst may be the strong HeI absorption line at 1.083 μm, observed at a velocity of  $v_{\text{LSR}} = 430 \text{ km s}^{-1}$  and displaying weak emission on the red side. Several hydrogen lines of V1647 Ori (H $\alpha$ , Pa $\beta$ , Pa $\gamma$ , Pa $\delta$ ) have also shown P Cygni profiles. While emission dominates the hydrogen lines, the emission component of the 1.083 μm HeI line is much weaker (see Fig. 2). The difference between H $\alpha$  and HeI line shapes suggests that the hydrogen lines originate from the larger volumes of the outer wind regions, whereas the HeI line, observed in absorption against a hot continuum, probes a much smaller volume of the innermost region of the wind.

Helium lines have not been observed in FUors, but are present in both EXor and T Tauri spectra. HeI requires hot environment ( $T = 12000 \text{ K}$ ), or a strong UV source to be excited. In T Tauri stars the origin of HeI emission is connected to the hot wind emanating from the stellar surface at the footpoints of magnetospheric accretion (Bastian et al. 2001). Tracers of accretion footpoints cannot be identified in FUor spectra. Mass infall into the stellar surface is supposed to proceed in these objects through an equatorial boundary layer whose structure is rather uncertain (e.g. Hartmann & Kenyon 1996; Hartmann, Hinkle & Calvet 2004).

The HeI line of V1647 Ori demonstrates the presence of a hot region in the star/disk system, and this region probably gained its high temperature from accretion shocks. The morphology of the line suggests an accretion/wind geometry different from magnetospherically accreting (T Tauri and EXor) stars. Given that the hot wind can be observed in absorption against a hot surface and that our line of sight tilts at some 30° to the equator of the star, we speculate that the wind traced by the HeI line is mostly equatorial, in contrast to the wind components observed in the hydrogen lines, and to those giving birth to the polar cavity.

#### 4.4. FUor or EXor?

Both types of outburst stars are thought to undergo rapid accretion, but the different structure of the circumstellar

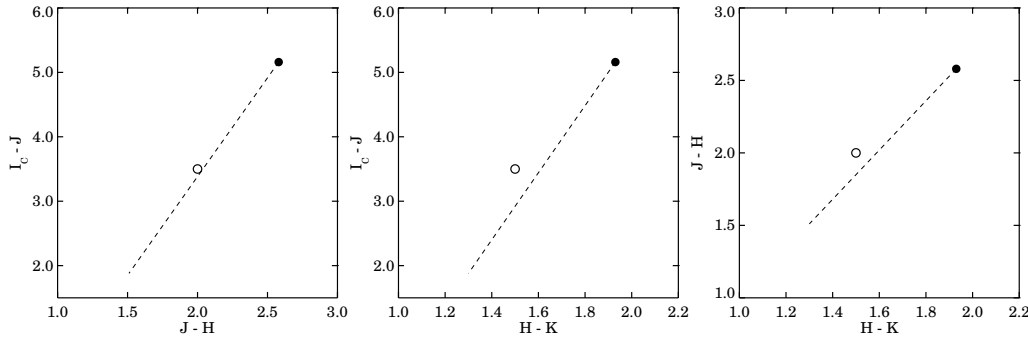


Fig. 8. Position of V1647 Ori in  $I_c - J$  vs.  $J - H$ ,  $I_c - J$  vs.  $H - K$ , and  $J - H$  vs.  $H - K$  colour-colour diagrams. Filled symbols mark published pre-outburst data (M A SS, B riceno et al 2004), and open symbols show post-outburst measurements of this work. The dashed lines represent extinction paths corresponding to  $A_V = 10$  mag.

lar environments results in different appearance of both types of object. The most striking differences are that while EXors appear extremely active, magnetospherically accreting T Tauri stars during their several-month-long outbursts, FUors appear as rapidly rotating supergiant stars, exhibit strong wind signatures, and their eruptions last several decades.

The P Cygni profiles of hydrogen lines distinguish V1647 Ori from the prototype EXor EX Lupi, whose Balmer lines exhibited inverse P Cygni profiles during outburst (Lehmann, Reipurth & Brandner 1995; Herbig et al. 2001). Inverse P Cygni profiles are common among the Paschen lines of T Tauri stars too (Folha & Emerson 2001). EXors show T Tauri-type spectra during outburst, while V1647 Ori has never shown a T Tauri-type spectrum. The morphology of the HeI 1.083 line is also different from that in EXors. Though HeI lines are absent from FUors, the typical shape of their H line is similar to this line, suggesting that the structure of the line-emitting region of V1647 Ori is similar to, but its temperature is higher than that in known FUors.

Inspecting the optical spectrum observed by B riceno et al. (2004) at the nebular position C (presented in their Fig. 4) one can recognize several features found in known FUors. H shows a P Cygni signature like the Paschen lines and H. The H line shows up as a broad absorption, and H is a still broader, double-bottomed absorption line. Similar line structure was found by Hartmann & Calvet (1995) in FU Ori: strong lines, formed in the outer regions of the system, had P Cygni profiles, while weak lines, formed in the inner regions showed broad, often double-bottomed absorption, consistent with the picture that the source of the spectrum is the surface of a rotating disk and stellar wind originating from the disk. Further FUor characteristics may be the structure of H and CaIIK. H is appreciably narrower than H and H, and, at the same time CaIIK can be seen in emission, but CaIIH cannot. Herbig, Petrov & Duemmler (2003) explained this spectral feature so that the blue part of the

broad H absorption is quenched by the CaIIH emission line. They stress that this feature is an important characteristic of FUors.

The SEDs of FUors indicate that, in addition to the accretion disks, dusty envelopes are present around the stars. Both the pre- and post-outburst SED of V1647 Ori resembles those of the known FUors (Abraham et al. 2004; Andrews et al. 2004). Moreover, the envelope can be identified in the J - H and H - K images of the environment of V1647 Ori.

FUor outbursts last longer than their EXor type counterparts. The time elapsed since the outburst of V1647 Ori is short for classification. The shape of the light curve, however, is more characteristic of FUors (Walter et al. 2004).

We believe, based on the above arguments, that we have been witnessing a FUor eruption of V1647 Ori. Several unusual observed features of the eruption, not found in other FUors, such as the infrared emission spectrum, may be related to the early phases of the outburst.

## 5. Conclusions

Comparison of our optical and near infrared data obtained in February/April 2004 on V1647 Ori with published results led to the following new results: (1) The overall fading of the star is probably smaller than the light curves of Walter et al. (2004) suggested. (2) The time delay between the light curves of V1647 Ori and the nebular clump C suggests that the inclination of the axis of the conical nebula to the line of sight is about 60°. (3) The colour distribution of the infrared nebula around V1647 Ori revealed a attenuated, dusty envelope perpendicular to the optical nebula. (4) Comparison of the  $K_s$  and  $R_c$  images of McNeil's nebula shows that HH22A consists of two physically different knots: the southern is a part of the nebula but not seen in the  $K_s$ , while the northern one is outside the illuminated region, but exhibits  $H_2$  2:12 mag emission. (5) We derived a visual extinction of  $A_V = 8.4$  mag from

the E ( $R_c - I_c$ ) colour excess of V1647 Ori. (6) We propose that the colour changes of V1647 Ori during the outburst resulted from temperature increase instead of the decrease of the visual extinction. In this case the amplitudes of the outburst were as follows:  $I - 5.4$  mag,  $J - 3.7$  mag,  $H - 3.2$  mag, and  $K_s - 2.8$  mag. (7) No clear evidence of magnetospheric accretion, characteristic of EXors, can be identified in the published optical and near infrared spectra of the star. On the contrary, several features characteristic of FUors do appear. Together with the light curve and SED the spectroscopic properties suggest that V1647 Ori is an FU Ori type star.

Acknowledgements. Financial support from the Hungarian OTKA grants T 34584 and T 37508 is acknowledged. AM, JAP, MCL and M JVN acknowledge support from grant AYA 2001-1658, funded by the Spanish Dirección General de Investigación. PA. acknowledges the support of the Bolyai Fellowship. Many thanks are due to Fernanda Arriaga and Gabriel Gómez for helping with the data collection at the IAC-80 telescope. We also thank Nicola Caon for his continuous help with all Iraf related questions.

## References

Abram P., Kospala A., Czerny Sz. et al. 2004, *A & A*, 419, L39

Acosta-Pulido J. A. et al. 2003, *ING Newsletter*, 7, 15

Andrews S. M., Rothberg B. & Simon T. 2004, *ApJ*, 610, L45

Beristain G., Edwards S. & Kwan J. 2001, *ApJ*, 551, 1037

Briceno C., Vivas A. K., Hernandez J., et al. 2004, *ApJ*, 606, L123

Cohen J. G., Frogel J. A., Persson S. E. & Elias J. H. 1982, *ApJ*, 249, 481

Elstob J. & Mundt R. 1997, *AJ*, 114, 280

Folha D. F. M. & Emerson J. P. 2001, *A & A*, 365, 90

Harker D., Bergman J., Tielens A. G. G. M., Terpstra B. & Rank D. 1997, *A & A*, 629, 640

Hartmann L. & Calvet N. 1995, *AJ*, 109, 1846

Hartmann L., Hinkle K. & Calvet N. 2004, *ApJ*, 609, 906

Hartmann L. & Kenyon S. J. 1996, *ARA & A*, 34, 207

Henden A. 2004, [http://spire.mit.edu/classes/phys440/lectures/new\\_star/mcneldat](http://spire.mit.edu/classes/phys440/lectures/new_star/mcneldat)

Herbig G. H. 1977, *ApJ*, 217, 693

Herbig G. H., Aspin C., Gilmore A. C., Imhoof C. L. & Jones A. F. 2001, *PA SP*, 113, 1547

Herbig G. H., Petrov P. P. & Duemmler R. 2003, *ApJ*, 595, 384

IPAC 2003, The 2MASS All Sky Catalog, [www.ipac.caltech.edu](http://www.ipac.caltech.edu)

Johnstone D., Finch M., Mitchell G. F. & Moriarty-Schieven G. 2001, *ApJ* 559, 307

Lancon A. & Rocca-Volmerange B. 1992, *A & AS*, 96, 593

Landolt A. U. 1992, *AJ*, 104, 340

Lehmann T., Reipurth B. & Brandner W. 1995, *A & A*, 300, L9

Manchado-Torres A. et al. 2003, in 'Instrument Design and Performance for Optical/Infrared Ground-based Telescopes,' Eds. Iye M., Morwood A., Proc. of the SPIE, 4841, 160

McNeil J. W. 2004, *IAUC*, 8284

Meyer M. R., Calvet N. & Hillenbrand L. A. 1997, *AJ*, 114, 288

Ojha D. K., Kusakabe N. & Tamura M. 2004, *IAUC*, 8306

Reipurth B. & Aspin C. 2004, *ApJ*, 606, L119

Rieke G. H. & Lebofsky M. J. 1985, *ApJ*, 288, 618

Samus N. N. 2004, *IAUC*, 8354

Sellgren K., Werner M. W. & Almandola L. J. *ApJS*, 102, 369

Vacca W. D., Cushing M. C., & Simon T. 2004, *ApJ*, 609, L29

Walter F. M., Stringfellow G. S., Sherry W. H. & Pollatou A. F. 2004, *AJ*, in press (astro-ph/0406618)